

LANGMUIR

Subscriber access provided by The Univ of Iowa Libraries

Article

The Role of Tris(2-carboxyethyl)phosphine Reducing Agent in the Controlled Formation of n,n -Alkanedithiols Monolayers on Au(111) with Monocoordinated and Bicoordinated Configurations

Esteban Matías Euti, Patricio Vélez Romero, Ezequiel Pedro Marcos Leiva, Vicente Antonio Macagno, Patricia A. Paredes-Olivera, Eduardo Martin Patrio, and Fernando Pablo Cometto

Langmuir, **Just Accepted Manuscript** • DOI: 10.1021/acs.langmuir.6b02079 • Publication Date (Web): 31 Aug 2016

Downloaded from <http://pubs.acs.org> on September 3, 2016

Just Accepted

“Just Accepted” manuscripts have been peer-reviewed and accepted for publication. They are posted online prior to technical editing, formatting for publication and author proofing. The American Chemical Society provides “Just Accepted” as a free service to the research community to expedite the dissemination of scientific material as soon as possible after acceptance. “Just Accepted” manuscripts appear in full in PDF format accompanied by an HTML abstract. “Just Accepted” manuscripts have been fully peer reviewed, but should not be considered the official version of record. They are accessible to all readers and citable by the Digital Object Identifier (DOI®). “Just Accepted” is an optional service offered to authors. Therefore, the “Just Accepted” Web site may not include all articles that will be published in the journal. After a manuscript is technically edited and formatted, it will be removed from the “Just Accepted” Web site and published as an ASAP article. Note that technical editing may introduce minor changes to the manuscript text and/or graphics which could affect content, and all legal disclaimers and ethical guidelines that apply to the journal pertain. ACS cannot be held responsible for errors or consequences arising from the use of information contained in these “Just Accepted” manuscripts.



ACS Publications

Langmuir is published by the American Chemical Society, 1155 Sixteenth Street N.W., Washington, DC 20036

Published by American Chemical Society. Copyright © American Chemical Society. However, no copyright claim is made to original U.S. Government works, or works produced by employees of any Commonwealth realm Crown government in the course of their duties.

1
2
3
4
5
6
7
8
9
10
11
12
13
14
15
16
17
18
19
20
21
22
23
24
25
26
27
28
29
30
31
32
33

The Role of Tris(2-carboxyethyl)phosphine Reducing Agent in the Controlled Formation of α,ω -Alkanedithiols Monolayers on Au(111) with Monocoordinated and Bicoordinated Configurations

34
35
36
37
38
39
40
41
42
43

*Esteban M. Euti,^a Patricio Vélez-Romero,^b Ezequiel P. M. Leiva,^b Vicente A. Macagno,^a Patricia
A. Paredes-Olivera,^b E. Martín Patrino^{a,*} and Fernando P. Cometto^{a,*}*

44
45
46
47
48
49
50
51
52
53
54
55

Instituto de Investigaciones en Físico Química de Córdoba (INFIQC) CONICET-UNC, a)
Departamento de Fisicoquímica and b) Departamento de Matemática y Física, Facultad de
Ciencias Químicas, Universidad Nacional de Córdoba, Ciudad Universitaria, X5000HUA
Córdoba Argentina.

56
57
58
59
60

KEYWORDS. Alkanedithiols, TCEP, Au (111), Reductive Desorption, DFT.

ABSTRACT

The addition of the reducing agent tris(2-carboxyethyl) phosphine (TCEP) during the formation of α,ω -alkanedithiols monolayers on Au(111) using the immersion method produces the assembly of monolayers with bicoordinated molecules (both S-terminal groups bound to the surface) that have a reductive desorption potential that is more positive than for monolayers with monocoordinated molecules in a standing up configuration. We show that the use of TCEP either during formation of the monolayer or as a post treatment procedure allows the controlled formation of monolayers with bicoordinated or monocoordinated configurations. Density Functional Theory (DFT) calculations were performed to elucidate the role of TCEP in the formation of the bicoordinated configuration. We investigated the TCEP-dithiol interaction in ethanol solvent as well as the coadsorption of trimethylphosphine with 1,2-ethanedithiol on Au(111). The Brønsted base character of the phosphine facilitates the H exchange from the $-SH$ groups of the dithiol to the phosphorous atom of TCEP with very low activation energy barriers, thus allowing the thiolate groups to bind to the Au(111) surface, thus yielding the bicoordinated configuration. Dithiol lifting mechanisms such as H exchange between S atoms and the formation of intra/inter layer disulfide bonds have much higher energy barriers.

INTRODUCTION

Self-assembled monolayers (SAMs) on solid surfaces are widely studied due to their potential applications in several areas such as corrosion inhibition, molecular recognition, nanoelectronics, biosensing, etc.¹⁻³

A SAM is built up of molecules made of three different parts: a head-group bonded to the surface, a spacer group responsible for intermolecular interactions and a terminal group that confers a new chemical identity to the modified surface. The most popular type of SAMs are those composed of alkanethiolates adsorbed upright on Au(111) surfaces; these SAMs can be prepared from either alkanethiols ($\text{CH}_3\text{-(CH}_2\text{)}_n\text{-SH}$) that deprotonate upon adsorption, or disulfides ($\text{((CH}_3\text{-(CH}_2\text{)}_n\text{-S)}_2$) which dissociate into two thiolates during adsorption.

Another interesting type of SAMs are those made of α,ω -alkanedithiols (DTs), i.e. carbon chains terminated with thiol groups in both ends ($\text{HS-(CH}_2\text{)}_n\text{-SH}$). DTs molecules may be adsorbed in a standing up (SU, mono-coordinated)⁴⁻⁶ or a lying-down (LD) configuration (bi-coordinated)^{7,8} depending on the preparation method. Bi-coordinated adsorption exposes the alkyl chain to the environment; whereas the mono-coordinated one only exposes, in principle, the -SH group. The synthesis of SH-terminated surfaces is of great interest because they have the potential ability of binding to two metallic entities, and serve, therefore, to connect nanoparticles or to bind them to a surface.⁹

The preparation procedure has an important influence on the surface structure and chemistry of SAMs of DTs on Au(111) as recently reviewed by Hamoudi et al.¹⁰ Ordered standing up monolayers exposing the -SH group were formed in n-hexane solution in the absence of light.¹¹⁻

¹⁴ The acetyl protection of one thiol end also allowed the formation of an -SH terminated surface.¹⁵ The formation of SU dithiols has also been reported to occur from vapor phase.¹⁶

1
2
3 However, a small amount of LD phase¹² as well as bicoordinated dithiols in a U-loop
4 configuration¹⁷ may also coexist with the SU phase. Short immersion times of a few seconds
5
6 produce LD structures of 1,5-pentanedithiol whereas at long immersion times the SU structure is
7
8 obtained.¹⁸ Under low flux and low dose conditions in adsorption experiments from vapor, LD
9
10 phases have been observed for and 1,4-benzenedimethanethiol¹⁶ and 1,4-butanedithiol.¹⁹ LD
11
12 phases of 1,4-butanedithiol were also observed from liquid phase assembly using millimolar
13
14 solutions of ethanol and hexane at room temperature (RT) on gold substrates.²⁰ DFT calculations
15
16 show that the LD → SU phase transition under vacuum conditions is favored as the hydrocarbon
17
18 chain length of DTs is increased.²¹ The parameters that control the thermodynamic stability of
19
20 the different phases are the binding energy of the adsorbates and the number of adsorbed species
21
22 per unit of substrate area.²¹
23
24
25
26
27
28

29 The presence of disulfide bonds has a profound influence on the structure of DT layers.
30
31 Interlayer S–S bonds are responsible for the formation of SU-multilayer structures whereas
32
33 intralayer S–S bonds may be present in a dithiol monolayer.^{5,6,22} Small chain DTs are more
34
35 reactive towards the formation of multilayers in the presence of O₂ by oxidation of –SH groups
36
37 to disulfides. This complicates the reproducible and controlled formation of DT monolayers.
38
39

40 Disulfide reducing agents may be employed to shave the multilayers leaving only a single
41
42 monolayer or they may be introduced in the forming solution containing the DT.²²⁻²⁶
43
44

45 XPS is a very powerful technique to elucidate the structure of dithiol layers as the S2p binding
46
47 energy has different values for the –SH terminal group, the disulfide S–S bond and the surface
48
49 S–Au bond.^{10,19,26} In a previous investigation using high resolution photoelectron spectroscopy
50
51 we found that tris(2-carboxyethyl) phosphine added to the forming solution leads to the
52
53 reproducible formation of lying down structures of α,ω -alkanedithiols irrespective of the chain
54
55
56
57
58
59
60

1
2
3 length and without the need of deoxygenating the forming solution.²⁶ This implies that the
4
5 phosphine not only inhibits the formation of disulfide bonds but also blocks the possible
6
7 mechanisms responsible for the LD → SU phase transition.
8
9

10 In the present work we investigated the mechanisms involved in the formation of lying-down
11
12 phases in the presence of TCEP. We considered 1,2-ethanedithiol (C2DT), 1,6-hexanedithiol
13
14 (C6DT), 1,8-octanedithiol (C8DT) and 1,9-nonanedithiol (C9DT). The theoretical calculations
15
16 were performed with C2DT. In the first part we use cyclic voltammetry as the potential of
17
18 reductive desorption current peaks is very sensitive to the monolayer structure. In the second part
19
20 we use density functional theory to investigate the TCEP-induced formation of a C2DT lying-
21
22 down structure by considering the a) the TCEP-C2DT interaction in the ethanolic forming
23
24 solution b) the energetics involved in the LD→SU transitions of C2DT molecules on Au(111)
25
26 and c) the coadsorption of trimethylphosphine with C2DT on Au(111).
27
28
29
30
31

32 **EXPERIMENTAL SECTION**

33
34
35 Chemicals. Dipping solutions were prepared using C2DT, C6DT, C8DT, C9DT, tris(2-
36
37 carboxyethyl)phosphine (TCEP) (Sigma-Aldrich) and absolute ethanol or *n*-hexane (Baker) as
38
39 solvents.
40
41

42
43 Gold Substrates. An Au crystal, 4 mm in diameter, oriented better than 1° towards the (111)-face
44
45 and polished down to 0.03 μm (MaTeck, Jülich, Germany) was used as a working electrode for
46
47 cyclic voltammetry. The cleaning of this substrate involved repeated cycles of annealing on a H₂
48
49 flame and cooling in a N₂ atmosphere. Au films (500 nm thick) evaporated on heat resistive
50
51 glasses were employed as substrates for the photoemission experiments. These substrates were
52
53 annealed several times in a butane flame for two minutes and cooled down to room temperature
54
55 in a stream of nitrogen.
56
57
58
59
60

1
2
3 SAM preparation. The self-assembled adlayers were prepared by immersing the gold substrates
4 into 0.2 mM solutions of dithiol in ethanol without deoxygenating. In one experiment, the
5 formation of the adlayer was also performed in an *n*-hexane solvent. The post deposition
6 treatment consisted in the immersion of the sample in a concentrated solution (20%:80%,
7 H₂O:ethanol) of TCEP during 10 minutes. When the reducing agent was added to the formation
8 bath, monolayers were formed by immersing the substrates into 0.2 mM of the corresponding
9 dithiol and 4.0 mM of TCEP ethanolic solutions for 24 h. After the adlayers were formed, the
10 substrates were washed several times with pure ethanol and Milli-Q water in order to remove
11 physisorbed species.
12
13
14
15
16
17
18
19
20
21
22
23

24
25 Electrochemical Measurements. Cyclic Voltammograms (CV) were performed with a Solartron
26 1260 electrochemical interface and a conventional electrochemical three electrode cell with
27 separate compartments for reference (Ag/AgCl (NaCl 3M)) and counter electrode (Pt wire).
28 Electrical contact with the working electrode was made by means of a meniscus on the surface of
29 the electrolytic solution. The electrolyte was thoroughly deoxygenated by bubbling with nitrogen
30 prior to each experiment. Reductive desorption experiments were performed in 0.1 M KOH
31 solutions.
32
33
34
35
36
37
38
39
40
41

42 THEORETICAL METHODS

43
44 The first-principles periodic calculations within the framework of density functional theory
45 (DFT) were performed with the SIESTA code.²⁷ Valence electrons were described with a set of
46 double-z polarized bases. The number of *k*-points in the *x-y* plane was increased to obtain
47 convergence in the system energy better than 0.002 eV/atom, resulting a sample of 3×3×1 *k*-
48 points finally. The separation in the *z* direction between the neighboring metal slabs (made of 4
49 layers (111) on a 3×3 unit cell) was ca. 20 Å to ensure convergence in the system energy. The
50
51
52
53
54
55
56
57
58
59
60

1
2
3 exchange and correlation effects were described using the generalized gradient approximation
4 GGA in the functional Perdew-Burke-Ernzerhof.²⁸ The energy shift used to confine the electrons
5
6 in the pseudoatomic orbitals was 0.02 eV.
7
8

9
10 We studied the minimum energy reaction paths connecting an optimized initial configuration to
11 the desired final structure by using the nudged elastic band (NEB) method.^{29,30} The progress
12 along the reaction pathway is represented by the so called reaction coordinate which is a
13 dimensionless quantity varying from 0 (reactants) to 1 (products).
14
15

16
17 The TCEP-dithiol interaction was investigated using the Gaussian 09 package.³¹ The solution-
18 phase geometry optimizations were performed using the PBE functional for both exchange and
19 correlation and 6-311++G(d,p) basis set.²⁸ The polarizable continuum model (PCM) was used to
20 describe solvent effects.³² Ethanol was used as the solvent.
21
22

23 24 25 26 27 28 29 **RESULTS AND DISCUSSION**

30 31 Electrochemical Characterization

32
33 Figure 1 shows cathodic sweep responses corresponding to C2DT gold modified samples
34 prepared by different procedures. As it can be seen, the electrochemical response is very
35 sensitive to the preparation method used.
36
37

38
39 The reductive desorption profile of a C2DT layer prepared after immersion for 24 hours in an
40 ethanolic C2DT (0.2 mM) solution (Figure 1a, black line) shows a main desorption peak at -913
41 mV with a pronounced broad shoulder shifted to more negative potential values. The second
42 scan (dashed line) presents two peaks, one close to the potential of the main peak and another
43 one at nearly the same potential as that of the shoulder of the first scan. The integrated area of the
44 first scan (colored in the Figure 1 a)) gives a desorption charge of around 200 $\mu\text{C cm}^{-2}$ which
45
46
47
48
49
50
51
52
53
54
55
56
57
58
59
60

represents more than twice the charge expected for the desorption of an ideal SU dithiolate monolayer ($75 \mu\text{C cm}^{-2}$).

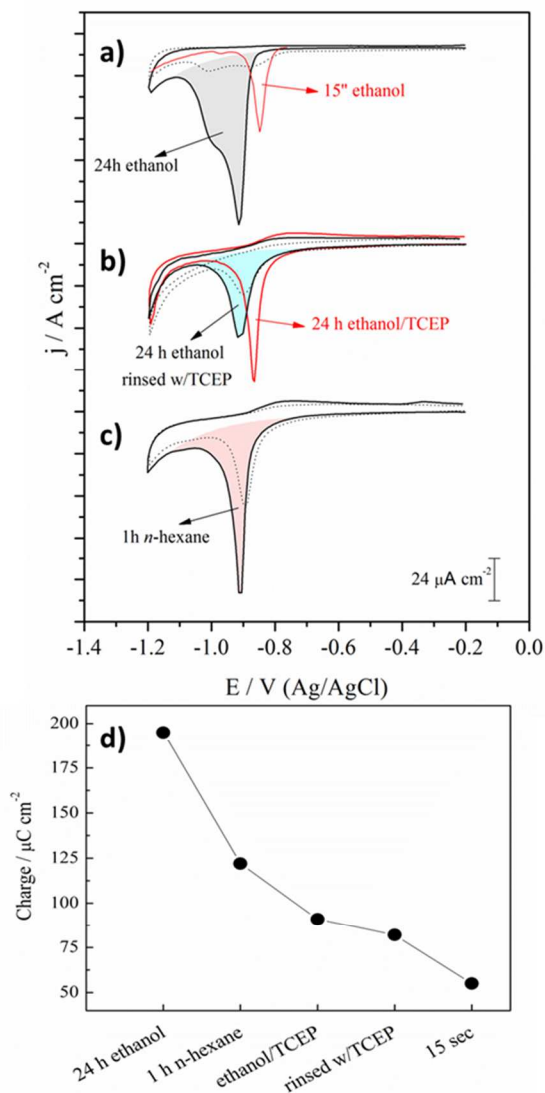


Figure 1. Reductive desorption profiles obtained for DTs-layers on Au(111) substrates prepared by different procedures. The solid curves correspond to the first potential scan and the dotted curves to the second potential scan. a) immersion for 15 sec (red curve) and 24 h (black curve) in ethanolic solutions; b) immersion for 24 h in ethanolic solution and post treatment with TCEP (black curve), and immersion for 24 h in ethanolic solution with TCEP in the forming solution (red curve); c) immersion for 1 h in a *n*-hexane solution; d) reductive desorption charge for the different preparation procedures. Electrolyte: KOH 0.1M. Scan rate: 50 mV/s.

1
2
3 Previous impedance²⁵ and XPS²⁶ measurements showed that after the immersion for 24h in a 0.2
4 mM C2DT-ethanol solution, a multilayer structure is formed, therefore the charge excess can be
5 attributed to the additional charge necessary to reduce inter/intralayer S–S bonds. The breakage
6 of S–S bonds and S–Au bonds seems to occur at similar potential values, a feature that prevents
7 the separate study of these reduction processes. The presence of a shoulder in the CV profile at
8 more negative potentials is consistent with the desorption of species with a lower solubility than
9 that of C2DT molecules, such as remaining C2DT-dimers formed by interlayer S–S bonds not
10 reduced in the main peak.
11
12

13 Haiss et al.¹⁸ showed by means of photoemission spectra that both S atoms of a DT molecule are
14 bonded to the gold surface when the formation procedure involves short immersion times. In
15 order to obtain an electrochemical reference of a low coverage LD structure, we investigated
16 different samples prepared by short immersion times. Figure 1 a) (red line) shows the cathodic
17 sweep of a gold sample modified by the immersion during 15 seconds in a diluted C2DT-
18 solution. This desorption profile exhibits a main desorption peak at –848 mV and a small hump
19 at more negative values. The charge involved in the desorption process ($55 \mu\text{C cm}^{-2}$) is lower
20 than that expected for an ideal SU monolayer ($75 \mu\text{C cm}^{-2}$) indicating a lower coverage of C2DT.
21 The shift of the desorption potential to a more positive value indicates weaker interactions
22 among the alkyl chains which is consistent with a low density LD structure. We interpret the
23 remarkable differences in the CV profiles of Figure 1 a) with the immersion time in the forming
24 solution as the transition from a low density LD monolayer to a SU multilayer structure.
25
26
27
28
29
30
31
32
33
34
35
36
37
38
39
40
41
42
43
44
45
46
47
48
49

50 An effective method to remove undesired S–S bonds is to use reducing agents (like
51 phosphines,^{22,24,25} β -ME or DTT²³) in some stage of the preparation procedure. In Figure 1 b),
52 two experiments accounting for the use of the TCEP reducing agent are shown. The first case
53
54
55
56
57
58
59
60

1
2
3 (black full line) represents the electrochemical characterization of a sample formed by the
4 immersion during 24 hours in a diluted C2DT-solution (as that described in Figure 1 a)) and then
5 immersed during 10 minutes in a 20 mM aqueous/ethanolic (20:80) solution of TCEP. The CV
6 profile obtained after the modification of the sample with this procedure exhibits a desorption
7 profile with a single peak at almost the same value (-917 mV) at which the main peak is
8 observed for the immersion of 24 h. Remarkably, the shoulder at more negative values
9 disappears completely and the charge involved in the reduction process decreases to $82 \mu\text{C cm}^{-2}$,
10 almost the charge expected for the desorption of an ideal SU monolayer.
11

12 The reducing agent was also used *during* the formation of the adlayer. We prepared an ethanolic
13 C2DT solution with a [TCEP]/[C2DT] concentration ratio of 20. The cathodic sweep after a 24
14 hour immersion time (Figure 1b, red line) shows a narrow single peak at -866 mV with a charge
15 of $91 \mu\text{C cm}^{-2}$. The desorption potential is very close to that obtained for the diluted monolayer
16 prepared by the short immersion time of 15 seconds (only a 18 mV difference) indicating that
17 both monolayers should have the same LD configuration.
18

19 The formation of disulfide bonds seems to be inhibited when *n*-hexane is used as solvent.¹² The
20 first (continuous line) and second (dashed line) CV's scans in Figure 1c) correspond to a C2DT
21 layer formed in *n*-hexane solution. The desorption profile of the first scan (black full line)
22 presents a sharp peak at -902 mV and a desorption charge of $122 \mu\text{C cm}^{-2}$. This charge is much
23 lower than the value of $200 \mu\text{C cm}^{-2}$ obtained when the layer was formed in ethanol indicating
24 that the formation of disulfide bonds is mostly inhibited.
25

26 Figure 1d summarizes all the reduction desorption charges obtained for the different preparation
27 procedures. The plot demonstrates the sensitivity of the surface structure on the experimental
28 conditions. It suggests that if the forming conditions can be appropriately controlled, the desired
29
30
31
32
33
34
35
36
37
38
39
40
41
42
43
44
45
46
47
48
49
50
51
52
53
54
55
56
57
58
59
60

1
2
3 surface layer structure can be obtained. This is best achieved with the use of TCEP. We note that
4
5 all the experiments involving TCEP are highly reproducible either when the reducing agent is
6
7 used during or after the formation of the adlayer.
8
9

10 The lying-down structure of alkanedithiol (C2DT, C6DT and C9DT) adlayers prepared by
11
12 addition of TCEP in the forming solution were verified in a previous XPS study.²⁶ In this work
13
14 we showed the prevalence of the 162 eV feature over the 163.3 eV and 163.5 eV components in
15
16 the S2p spectra of samples incubated with TCEP in the alkanedithiol solution. The component at
17
18 162 eV is attributed to electrons emitted from thiolate-S atoms at the interface with the Au
19
20 substrate,³³⁻³⁶ whereas recent works attributed the components at 163.1-163.3 eV and 163.5 eV
21
22 to the presence of -SH and S-S groups, respectively^{10,14,19,26}. Thus, the clear prevalence of the
23
24 component at 162 eV proves the lying-down configuration of alkanedithiol adlayers and this
25
26 trend seems to be general as it observed for alkanedithiols with different chain length.²⁶
27
28
29
30

31 The capability of TCEP to control the monolayer structure was confirmed for longer chain
32
33 alkanedithiols as shown in Figure 2. In one set of experiments the monolayers were prepared
34
35 with TCEP in the forming solution and in another set the freshly prepared monolayers were post
36
37 treated with TCEP. We observed the same trend as for C2DT: the monolayers prepared with
38
39 TCEP have reductive desorption current peaks at more positive potentials than the monolayers
40
41 prepared without TCEP. In the first case the peak potentials are -955 mV, -960 mV and -952 mV
42
43 for C6DT, C8DT and C9DT, respectively; whereas in the second case they are -1031 mV, -1056
44
45 mV and -1062 mV, respectively.
46
47
48
49
50
51
52
53
54
55
56
57
58
59
60

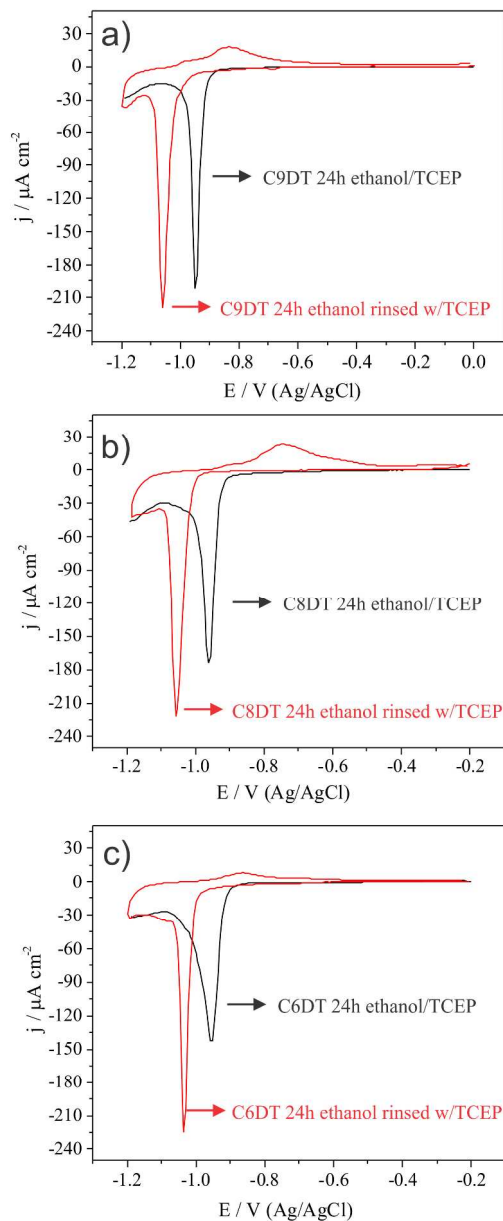


Figure 2. Reductive desorption profiles obtained for a) C9DT, b) C8DT and c) C6DT. The CV profiles in black correspond to monolayers prepared by 24 h immersion in ethanolic solution *with* TCEP. CV profiles in red correspond to monolayers prepared by 24 h immersion in ethanolic solution and post treatment with TCEP. Electrolyte: KOH 0.1M. Scan rate: 50 mV/s.

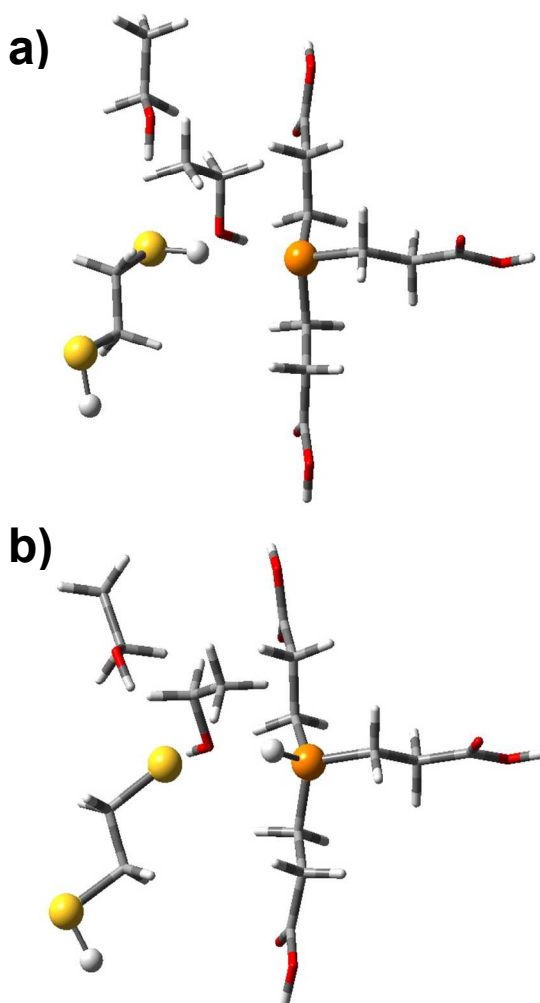
1
2
3 The most positive reductive desorption potential observed for the monolayers prepared with
4 TCEP is consistent with our previous photoelectron spectroscopy study which shows that these
5 monolayers are coordinated to the surface via both S atoms,²⁶ probably in a U loop
6 configuration. On the other hand, the monolayers prepared without TCEP in the forming solution
7 which have a standing up configuration²⁶ which maximized van der Waals interactions among
8 the alkyl chains, have the most negative reductive desorption potentials. It has been reported that
9 poor quality SAMs are obtained when the self assembly is performed in ethanol solvent.¹⁰ The
10 present results show that even for this challenging solvent, well ordered dithiol phases are
11 obtained when TCEP is used in the forming solution.
12
13
14
15
16
17
18
19
20
21
22
23

24 Density Functional Theory Calculations

25
26 The above results motivated us to investigate the mechanism by which only LD monolayers are
27 produced when TCEP is introduced in the forming solution. We therefore considered a) the
28 dithiol-TCEP interaction in the ethanol solvent, b) possible lifting mechanisms of LD dithiol
29 molecules on Au(111) and c) the phosphine-dithiol interaction when both species are coadsorbed
30 on the Au(111) surface.
31
32
33
34
35
36
37
38

39 Tris(2-carboxyethyl) phosphine acts as a Brønsted base which can abstract a proton from the
40 -SH group giving rise to thiolate-phosphonium ion pairs. Phosphorus has a relatively large
41 polarizability and thus can stabilize charged intermediates.³⁷⁻³⁹ Figure 3a shows the C2DT-TCEP
42 structure before deprotonation of one of the -SH groups. The calculation was performed using
43 the Polarizable Continuum Model with ethanol as the solvent and we also included explicitly two
44 ethanol molecules as shown in Figure 3a. The equilibrium structure for the phosphonium cation-
45 thiolate anion complex is shown in Figure 3b. The thiolate anion is stabilized by the hydrogen
46 bonds (HB) of the two ethanol molecules. The HB bond length is 2.11 Å. The O atom of one of
47
48
49
50
51
52
53
54
55
56
57
58
59
60

1
2
3 the ethanol molecules is also involved in the HB with the protonated phosphonium cation with a
4 short HB bond length of 1.94 Å. The ΔE value for the deprotonation process is endothermic with
5
6 short HB bond length of 1.94 Å. The ΔE value for the deprotonation process is endothermic with
7
8 0.34 eV. An equivalent calculation with only one explicit ethanol molecule gives $\Delta E = 0.58$ eV
9
10 whereas the ΔE value in vacuum is 1.0 eV. These data show the stabilizing effect of the solvent
11
12 on the charged ions. The addition of more ethanol molecules is therefore expected to further
13
14 decrease the ΔE value. This shows that the deprotonation of the dithiol by TCEP is a kinetically
15
16 facile process.
17
18
19
20



55
56 **Figure 3.** a) Equilibrium structure of TCEP with 1,2-ethanedithiol and two ethanol molecules in
57 ethanol solvent. b) Equilibrium structure in ethanol solvent of the ion pair after the proton
58
59
60

1
2
3 transfer from the $-SH$ group of the dithiol to the P atom of TCEP. The OH groups of both
4 ethanol molecules form hydrogen bonds with the thiolate anion. For clarity, only the relevant
5 atoms are explicitly shown.
6
7
8
9

10
11 This fact, together with the high TCEP/dithiol concentration ratio of 20, implies that a fraction of
12 dithiols will be present in the anionic form in the ethanolic forming solution. Anions have strong
13 electrostatic interactions with metal surfaces mainly arising from the metal polarization. In
14 previous works we calculated the interaction of different anions with metal surfaces.^{40,41} The
15 sulfate anion (having nearly the same charge to mass ratio as the ethanedithiolate dianion), for
16 example, has a strong interaction of 6.24 eV with the Au(111) surface. In the case of the
17 ethanedithiolate dianion with the negative charges localized at both ends of the molecule, image-
18 charge interactions with the metal surface are maximized when the molecule adsorbs flat on the
19 surface. Therefore, there is a strong driving force for the ethanedithiolate anions to adsorb in a
20 low-lying configuration on the surface.
21
22
23
24
25
26
27
28
29
30
31
32
33

34 Phosphines also interact with the gold surface via the lone electron pairs on the phosphorous
35 atom. An STM investigation of trimethylphosphine on Au(111) showed that the interaction
36 strong enough to lift the gold herringbone reconstruction⁴² but was not so strong to eject
37 additional atoms and create etch pits, as is the case of alkanethiols. Therefore, under a
38 TCEP/C2DT ratio of 20 in the forming solution, the gold surface is expected to be initially
39 covered by TCEP molecules.
40
41
42
43
44
45
46
47

48 Due to the large size of the TCEP molecule, we used trimethylphosphine as a model to
49 investigate the reactivity of coadsorbed phosphine and dithiol molecules on Au(111) surface. We
50 calculated the energy profile for the deprotonation of a $-SH$ group (Figure 4a) of ethanedithiol
51 interacting with trimethylphosphine on Au(111). The corresponding structures for the reactants,
52
53
54
55
56
57
58
59
60

1
2
3 transition state and products are shown in the panels of Figure 4b. Panel I in Figure 4b shows the
4 equilibrium structure of the phosphine-dithiol complex on Au(111). 1,2-ethanedithiol adsorbs
5 with an S atom located on top of an Au atom whereas its H atom points towards the P atom of
6 trimethylphosphine as a consequence of the H-bond interaction. The adsorption of this complex
7 on the surface from vacuum is exothermic with $\Delta E = -0.51$ eV. In the transition state (panel II in
8 Figure 4b) the H atom has been transferred to the P atom and in the final state the phosphonium
9 cation adsorbs on the surface (panel III) with the PH group located on a hollow site. The energy
10 profile in Figure 4a shows that the hydrogen abstraction has a small energy barrier of 0.21 eV
11 whereas the reaction has $\Delta E = 0.0$. Considering as a reference the energy of the phosphine-dithiol
12 complex in vacuum, the whole reaction has $\Delta E = -0.506$ eV.
13
14
15
16
17
18
19
20
21
22
23
24
25
26

27 In summary, the deprotonation of the dithiol by the phosphine molecule is favored on the surface
28 with respect to the solution phase. For the sake of simplicity in Figure 4 we only considered the
29 interaction of one of the -SH groups of the dithiol with a phosphine molecule, but in a solution
30 with a phosphine concentration higher than that of the dithiol, the complex is expected to have a
31 phosphine molecule at both ends of the dithiol thus leaving lying-down dithiolate species
32 adsorbed on the surface.
33
34
35
36
37
38
39
40
41
42
43
44
45
46
47
48
49
50
51
52
53
54
55
56
57
58
59
60

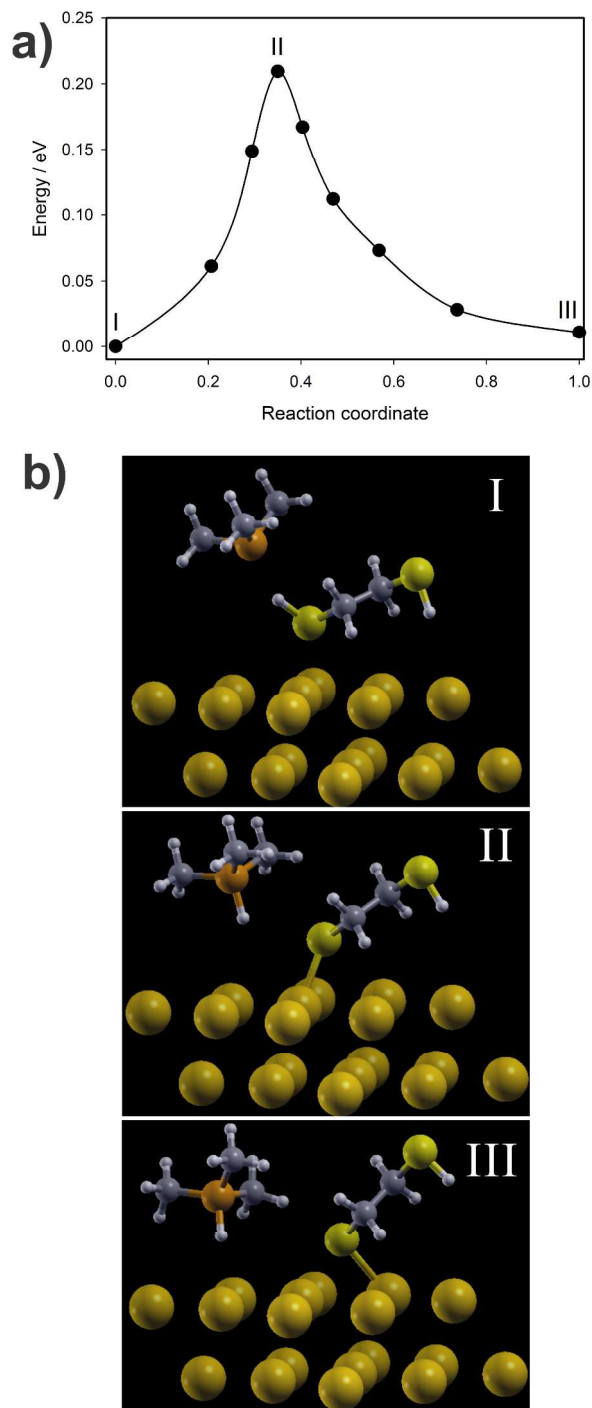
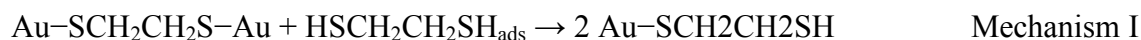


Figure 4. a) Energy profile for the H transfer from a $-SH$ group of 1,2-ethanedithiol to the P atom of trimethylphosphine. b) Equilibrium structures of phosphine-dithiol complex (panel I), transition state (panel II) and phosphonium-thiolate complex (panel III) on Au(111).

1
2
3 The high stability of the LD phase in the presence of TCEP observed experimentally indicates
4 that any mechanism involved in the LD \rightarrow SU transition is inhibited by the phosphine. It has
5 been proposed that this transition may originate from the proton transfer from the $-\text{SH}$ group of a
6 DT molecule approaching the surface to a DT molecule adsorbed flat on the surface. This
7 produces both the lifting of one end of the adsorbed molecule and the adsorption of the free DT
8 molecule through the deprotonated head-group, thus leading to two SU chemisorbed dithiol
9 molecules.^{3,12,13} We therefore addressed the energetics involved in the LD \rightarrow SU transition
10 considering three cases: the H-exchange mechanism (which we will denote with I), and two
11 disulfide mediated mechanisms (II and III). In all cases we considered the reaction of a LD 1,2-
12 ethyldithiolate with I) an adsorbed 1,2-ethyldithiol molecule, II) a monocoordinated SU
13 dithiolate (with an S atom bonded to the Au surface and an $-\text{SH}$ termination) and III) another LD
14 1,2-ethyldithiolate species.

15
16
17
18
19
20
21
22
23
24
25
26
27
28
29
30
31
32
33
34
35
36
37
38
39
40
41
42
43
44
45
46
47
48
49
50
51
52
53
54
55
56
57
58
59
60

Figures 5a shows the energy profiles for the three mechanisms and Figures 5b-d show the
corresponding initial, transition state and final structures. Mechanism I corresponds to the
following reaction:



where the bicoordinated dithiolate reacts with an adsorbed dithiol molecule to yield two standing
up dithiolates. The energy profile in Figure 5a shows that this mechanism has an energy barrier
of 0.68 eV. Thus, the H-exchange mechanism gives an energy barrier lower than that for the
S-H bond breakage (0.8 eV)⁴³ during adsorption of alkanethiols on the surface. Therefore, the
H-exchange seems to be a likely mechanism for the LD \rightarrow SU transition of alkanedithiols.
However, this mechanism cannot explain the substitution and lifting of LD dithiol molecules

mediated by dialkyl disulfide molecules⁴⁴ where there are no protons to transfer. In this case the only possibility is the formation of inter/intralayer S–S bonds.

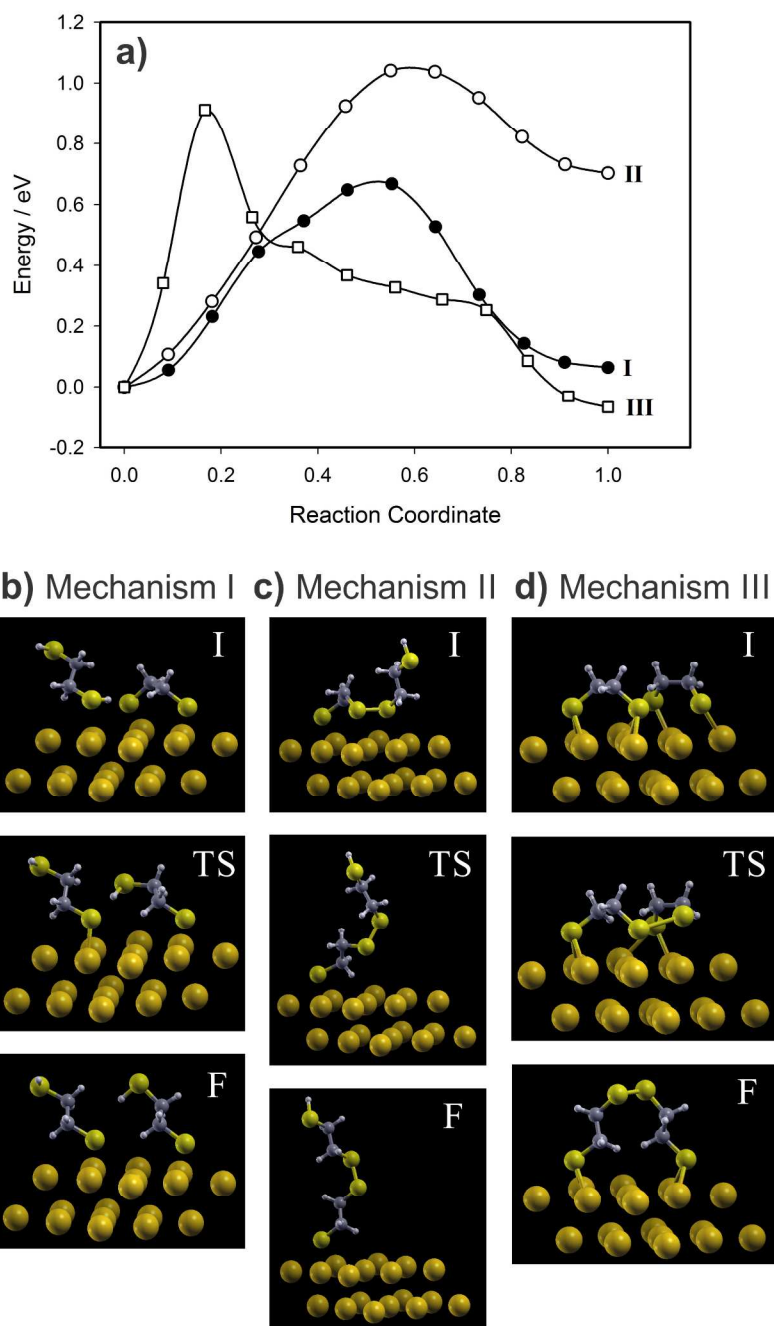
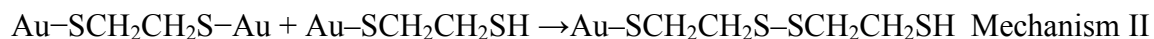


Figure 5. a) Energy profiles for 1,2-ethanedithiol lifting mechanisms (labeled I, II and III). Initial, transition state and final structures for b) H-exchange mechanism c) interlayer disulfide lifting mechanism and d) intralayer disulfide lifting mechanism.

1
2
3
4
5
6 We considered two mechanisms by which the formation of S–S bonds may be involved in the
7
8 lifting of LD dithiol molecules. They lead to the formation of interlayer and intralayer disulfide
9
10 bonds. In mechanism II, a surface disulfide bond is initially formed by the reaction of a SU
11
12 monocoordinated dithiol with one end of a LD bicoordinated dithiol:



14
15
16
17 The initial state in Figure 5c shows the structure of the resulting surface disulfide thus formed.

18
19
20 This reaction (not shown in Figure 5) has an energy barrier of 0.86 eV. In the next step, shown in
21
22 Figure 5c, the disulfide moiety desorbs from the surface yielding an interlayer disulfide bond.

23
24
25 This step has an energy barrier of 1.05 eV (Figure 5a) and involves the formation of a SU
26
27 bilayer.

28
29 The third mechanism comprises the formation of a monolayer with intralayer S–S bonds.^{5,6,25} It
30
31 involves the reaction between two neighboring DT in a LD configuration to form a S–S bond
32
33 according to:



35
36
37 As shown in Figure 5a, this process has an energy barrier of 0.91 eV.

38
39
40 The presence of intralayer S–S bonds is expected to introduce disorder in the monolayer
41
42 structure and it may be responsible for the lack of structure at the nanoscale observed in STM.^{5,45}

43
44
45 The formation of surface disulfide bonds from the lifting of LD dithiols as shown in Figure 5d
46
47 implies that the surface concentration of disulfide bonds should decrease with the increase of the
48
49 chain length of disulfides, as saturation coverage falls progressively with the chain length. This is
50
51 in agreement with our previous electrochemical measurements^{5,25} which show that the surface
52
53 concentration of S–S bonds effectively decreases as the alkyl chain length increases. Thus, the
54
55
56
57
58
59
60

1
2
3 mechanism represented in Figure 5d describes a situation in which intralayer S–S bonds can be
4
5 formed both in vacuum and in solution phase without the need of disulfide precursors, such as
6
7 O₂.
8
9

10 We can now address the role of TCEP in producing only lying-down structures. In the first place,
11 mechanisms involving disulfide bonds in LD → SU transitions are inhibited as TCEP is an
12 effective reducing agent of disulfides. In the second place, the H-exchange mechanism is not
13 expected to be operative because the H transfer from terminal –SH groups to the P atom of
14 phosphines has much lower energies than to the S atoms of adsorbed dithiolates. In the latter
15 case, the energy barrier of 0.21 eV (Figure 4a) is much lower than the barrier of 0.68 eV for the
16 H transfer between a free dithiol molecule and adsorbed thiolates (Figure 5a).
17
18
19

20 Most applications involving dithiols require a compact SU monolayer with terminal –SH groups
21 exposed to the solution. In this context, the post treatment with TCEP assures the formation of a
22 single monolayer as it reduces interlayer disulfide bonds. This was clearly shown for the case of
23 the reactive C2DT which has a high tendency to form multilayers.
24
25
26

27 The alkyl chain of a dithiol may have –NH₂ or –OH functionalities⁴⁶ which for certain
28 applications are required to interact with the medium. An example is the use of dithiothreitol, for
29 which the exposure of the –OH groups in the lying-down configuration produces a
30 biocompatible monolayer.⁴⁷ For this case, the formation of a monolayer with bicoordinated
31 molecules may benefit from the use of TCEP during the formation of the monolayer.
32
33
34
35

36 Although the uncontrolled formation of lying down dithiol structures is to be avoided in most
37 applications, the TCEP induced formation of compact bicoordinated molecules should be
38 considered as a platform for the further development of complex nanostructures by inducing the
39 LD to SU phase transitions using temperature or other perturbations.
40
41
42
43
44
45
46
47
48
49
50
51
52
53
54
55
56
57
58
59
60

1
2
3 It has been shown that a lying-down phase of butanedithiol (C4DT) may be removed by the
4 immersion in a didodecyl disulfide solution in n-hexane.⁴⁴ Our calculations give some insights
5 on the mechanisms which may be involved in the replacement of C4DT by a SU phase of
6 dodecanethiolate (C12T), resulting from the breakage of the S–S bond of the dialkyldisulfide. In
7 the case of dimethyldisulfide, the energy barrier for the breakage of the S–S bond on Au(111) is
8 0.6 eV on average^{48,49} and similar values are expected for other disulfides. This implies that upon
9 adsorption, the dialkyldisulfide may exist as an intermediate but it will finally dissociate at RT in
10 laboratory time. The direct desorption C4DT into the n-hexane solvent is a very unlikely
11 mechanism as it involves the breakage of two S-Au bonds of around 1.8 eV⁴⁸ whereas the energy
12 gain due to the solvation of the molecule is small. We therefore envisage the following
13 mechanism for the displacement of C4DT molecules by the dialkyldisulfide. First, the growth of
14 SU domains of dodecanethiolate (originated by the dissociative adsorption of didodecyl
15 disulfide) is expected to initiate in disordered regions between the LD domains of C4DT.
16
17 Second, we think that the growth of these domains will induce the LD → SU transition of C4DT
18 molecules, thus leaving free surface area for the formation of more S-Au bonds. The increase in
19 the number of S-Au bonds per unit area²¹ and the development of vdW interactions between the
20 alkyl chains are the main driving forces for the growth of SAMs.

21
22 In this context, the LD → SU transition of C4DT molecules via the formation of a disulfide bond
23 (mechanism III in Figure 5) helps to free up space and has no energetic cost as it is an
24 exothermic reaction. If the disulfide formation reaction occurs again for the same pair of C4DT
25 species, a cyclic dimeric disulfide is formed on the surface. The binding energy of disulfide
26 molecules is very low (0.28 eV for dimethyldisulfide⁴⁸, for example) and therefore, an adsorbed
27 disulfide species may readily dissolve in the n-hexane solvent. In the particular case of C4DT,
28
29
30
31
32
33
34
35
36
37
38
39
40
41
42
43
44
45
46
47
48
49
50
51
52
53
54
55
56
57
58
59
60

1
2
3 the cyclic monomeric disulfide is a very stable six-membered molecule.⁵⁰ The adsorption of
4
5 dodecanethiolate molecules may also induce a transition from LD to U-looped C4DT molecules.
6
7
8 This step is expected to have a small energy barrier as the C4DT molecules remain bicoordinated
9
10 to the surface via both S-Au bonds. The next step would correspond to the breaking of the
11
12 surface bonds and the formation of the cyclic six-membered disulfide which may then dissolve.
13
14
15 For the latter reaction step we expect a similar energy barrier to that in mechanism III in Figure
16
17
18 5.
19

20 CONCLUSIONS

21
22 The addition of TCEP to the forming solution produces monolayers of α,ω -alkanedithiols which
23
24 are coordinated to the Au surface via both S atoms in agreement with our previous high
25
26 resolution photoelectron spectroscopy study.²¹ The monolayers with bicoordinated dithiol
27
28 molecules have reductive desorption potentials that are more positive than for monolayers with
29
30 SU monocoordinated molecules. Therefore, the use of TCEP either during formation of the
31
32 monolayer or as a post treatment procedure allows the precise control of the structure of
33
34 alkanedithiols with high reproducibility, yielding bicoordinated or monocoordinated
35
36 configurations, respectively.
37
38
39

40
41 DFT calculations were performed to elucidate the role of TCEP in the formation of bicoordinated
42
43 dithiol structures. We investigated the mechanisms involved in the LD \rightarrow SU transition of 1,2-
44
45 ethanedithiol as well as the reactivity of tris(2-carboxyethyl) phosphine with 1,2-ethanedithiol in
46
47 ethanol solvent and of trimethylphosphine with 1,2-ethanedithiol on the Au(111) surface.
48
49

50
51 The energy barriers for the mechanisms which may be involved in the LD to SU structural
52
53 transition (H transfer between adjacent S atoms and formation of disulfide bonds) are in the
54
55
56
57
58
59
60

1
2
3 range of 0.7-1.0 eV indicating that in principle they may all be feasible, with the H transfer
4
5 mechanism having the lowest barrier of 0.68 eV.
6
7

8 However, these mechanisms are inhibited in the presence of phosphines. The Brønsted base
9
10 behavior of TCEP may deprotonate the terminal –SH groups of the dithiol with a ΔE value lower
11
12 than 0.34 eV in ethanol solvent. When trimethylphosphine is coadsorbed with 1,2-ethanedithiol
13
14 on Au(111), the deprotonation has an energy barrier of only 0.21 eV, indicating that this process
15
16 is favored on the surface, thus leaving the molecule in a LD conformation with both thiolates
17
18 bound to the gold surface.
19
20
21

22 **ACKNOWLEDGMENTS**

23
24
25 This work was supported by CONICET (PIP grants 112-200801-000983 and 112-20080100958),
26
27 FONCyT (PICT grant 2014-2199).
28
29
30

31 **AUTHOR INFORMATION**

32 **Corresponding Authors**

33
34
35
36 * Prof. Fernando P. Cometto. e-mail: fcometto@fcq.unc.edu.ar.
37

38
39 * Prof. E. Martín Patrito. e-mail: martin@fcq.unc.edu.ar.
40

41 **Author Contributions**

42
43
44 The manuscript was written through contributions of all authors. All authors have given approval
45
46 to the final version of the manuscript.
47
48

49 **REFERENCES**

50
51
52 (1) Schreiber, F. Structure and growth of self-assembling monolayers. *Progr. Surf. Sci.* **2000**,
53
54 *65*, 151-256.
55
56
57
58
59
60

- 1
2
3 (2) Love, J. C.; Estroff, L. A.; Kriebel, J. K.; Nuzzo, R. G.; Whitesides, G. M. Self-Assembled
4 Monolayers of Thiolates on Metals as a Form of Nanotechnology. *Chem. Rev.* **2005**, *105*,
5 1103–1169.
6
7 (3) Vericat, C.; Vela, M. E.; Benitez, G.; Carro, P.; Salvarezza, R. C. Self-Assembled
8 Monolayers of Thiols and Dithiols on Gold: New Challenges for a Well-Known System. *Chem.*
9 *Soc. Rev.* **2010**, *39*, 1805–1834.
10
11 (4) Rieley, H.; Kendall, G. K.; Zemicael, F. W.; Smith, T. L.; Yang, S. X-Ray Studies of Self-
12 Assembled Monolayers on Coinage Metals. 1. Alignment and Photooxidation in 1,8-
13 Octanedithiol and 1-Octanethiol on Au. *Langmuir* **1998**, *14*, 5147–5153.
14
15 (5) Esplandiu, M. J.; Carot, M. L.; Cometto, F. P.; Macagno, V. A.; Patrito, E. M.
16 Electrochemical STM Investigation of 1,8-Octanedithiol Monolayers on Au(111): Experimental
17 and Theoretical Study. *Surf. Sci.* **2006**, *600*, 155–172.
18
19 (6) Carot, M. L.; Esplandiu, M. J.; Cometto, F. P.; Patrito, E. M.; Macagno, V. A. Reactivity of
20 1,8-Octanedithiol Monolayers on Au(111): Experimental and Theoretical Investigation. *J.*
21 *Electroanal. Chem.* **2005**, *579*, 13–23.
22
23 (7) Joo, S. W.; Han, S. W.; Kim, K. Adsorption of 1,4-Benzenedithiol on Gold and Silver
24 Surfaces: Surface-Enhanced Raman Scattering Study. *J. Colloid Interface Sci.* **2001**, *240*, 391–
25 399.
26
27 (8) Leung, T. Y. B.; Gerstenberg, M. C.; Lavrich, D. J.; Scoles, G.; Schreiber, F.; Poirier, G. E.
28 1,6-Hexanedithiol Monolayers on Au(111): A Multitechnique Structural Study. *Langmuir* **2000**,
29 *16*, 549–561.
30
31 (9) Cui, X. D.; Primak, A.; Zarate, X.; Tomfohr, J.; Sankey, O. F.; Moore, A. L.; Moore, T. A.;
32 Gust, D.; Harris, G.; Lindsay, S. M. Reproducible Measurement of Single-Molecule
33 Conductivity. *Science* **2001**, *294*, 571–574.
34
35 (10) Hamoudi, K.; Esaulov, V. A. Selfassembly of α,ω -dithiols on surfaces and metal dithiol
36 heterostructures. *Ann. Phys. (Berlin)* **2016**, *528*, 242–263.
37
38 (11) Hamoudi, H.; Guo, Z.; Prato, M.; Dablemont, C.; Zheng, W. Q.; Bourguignon, B.; Canepa,
39 M.; Esaulov, V. A. On the Self Assembly of Short Chain Alkanedithiols. *Phys. Chem. Chem.*
40 *Phys.* **2008**, *10*, 6836–6841.
41
42 (12) Millone, M. A. D.; Hamoudi, H.; Rodríguez, L.; Rubert, A.; Benítez, G. A.; Vela, M. E.;
43 Salvarezza, R. C.; Gayone, J. E.; Sánchez, E. A.; Grizzi, O.; *et al.* Self-Assembly of
44 Alkanedithiols on Au(111) from Solution: Effect of Chain Length and Self-Assembly
45 Conditions. *Langmuir* **2009**, *25*, 12945–12953.
46
47 (13) Hamoudi, H.; Prato, M.; Dablemont, C.; Cavalleri, O.; Canepa, M.; Esaulov, V. A. Self-
48 Assembly of 1,4-Benzenedimethanethiol Self-Assembled Monolayers on Gold. *Langmuir* **2010**,
49 *26*, 7242–7247.
50
51
52
53
54
55
56
57
58
59
60

- 1
2
3 (14) Pasquali, L.; Terzi, F.; Seeber, R.; Nannarone, S.; Datta, D.; Dablemont, C.; Hamoudi, H.;
4 Canepa, M.; Esaulov, V. A. UPS, XPS, and NEXAFS Study of Self-Assembly of Standing 1,4-
5 Benzenedimethanethiol SAMs on Gold. *Langmuir* **2011**, *27*, 4713–4720.
6
7
8 (15) Lau, K. H. A.; Huang, C.; Yakovlev, N.; Chen, Z. K.; O'Shea, S. J. Direct Adsorption and
9 Monolayer Self-Assembly of Acetyl-Protected Dithiols *Langmuir* **2006**, *22*, 2968–2971.
10
11 (16) Alarcón, L. S.; Chen, L.; Esaulov, V. A.; Gayone, J. E.; Sánchez, E. A.; Grizzi, O. Thiol
12 Terminated 1,4-Benzenedimethanethiol Self-Assembled Monolayers on Au(111) and InP(110)
13 from Vapor Phase. *J. Phys. Chem. C* **2010**, *114*, 19993–19999.
14
15 (17) Kohale, S.; Molina, S. M.; Weeks, B. L.; Khare, R.; Hope-Weeks, L. J. Monitoring the
16 Formation of Self-Assembled Monolayers of Alkanedithiols Using a Micromechanical
17 Cantilever Sensor. *Langmuir* **2007**, *23*, 1258–1263.
18
19 (18) Haiss, W.; Nichols, R. J.; Zalinge, H. van; Higgins, S. J.; Bethell, D.; Schiffrin, D. J.
20 Measurement of Single Molecule Conductivity Using the Spontaneous Formation of Molecular
21 Wires. *Phys. Chem. Chem. Phys.* **2004**, *6*, 4330–4337.
22
23 (19) Jia, J.; Mukherjee, S.; Hamoudi, H.; Nannarone, S.; Pasquali, L.; Esaulov, V. A. Lying-
24 Down to Standing-Up Transitions in Self Assembly of Butanedithiol Monolayers on Gold and
25 Substitutional Assembly by Octanedithiols *J. Phys. Chem. C* **2013**, *117*, 4625–4631.
26
27 (20) Millone, M. A. D.; Hamoudi, H.; Rodríguez, L.; Rubert, A.; Benítez, G. A.; Vela, M.
28 E.; Salvarezza, R. C.; Gayone, J. E.; Sánchez, E. A.; Grizzi, O. Self-assembly of alkanedithiols on
29 Au(111) from solution: Effect of chain length and self-assembly
30 conditions *Langmuir* **2009**, *25*, 12945–12953
31
32 (21) Carro, P.; Creus, A. H.; Muñoz, A.; Salvarezza, R. C. On the Thermodynamic Stability of
33 α,ω -Alkanedithiols Self-Assembled Monolayers on Unreconstructed and Reconstructed Au(111).
34 *Langmuir* **2010**, *26*, 9589–9595.
35
36 (22) Liang, J.; Rosa, L. G.; Scoles, G. Nanostructuring, Imaging and Molecular Manipulation of
37 Dithiol Monolayers on Au(111) Surfaces by Atomic Force Microscopy. *J. Phys. Chem. C* **2007**,
38 *111*, 17275–17284.
39
40 (23) Lundgren, A. O.; Björefors, F.; Olofsson, L. G. M.; Elwing, H. Self-Arrangement Among
41 Charge-Stabilized Gold Nanoparticles on a Dithiothreitol Reactivated Octanedithiol Monolayer.
42 *Nano Lett.* **2008**, *8*, 3989–3992.
43
44 (24) Weckenmann, U.; Mittler, S.; Naumann, K.; Fischer, R. A. Ordered Self-Assembled
45 Monolayers of 4,4'-Biphenyldithiol on Polycrystalline Silver: Suppression of Multilayer
46 Formation by Addition of Tri-N-Butylphosphine. *Langmuir* **2002**, *18*, 5479–5486.
47
48 (25) Cometto, F. P.; Calderón, C. A.; Euti, E. M.; Jacquelin, D. K.; Pérez, M. A.; Patrino, E. M.;
49 Macagno, V. A. Electrochemical Study of Adlayers of α,ω -Alkanedithiols on Au(111):
50 Influence of the Forming Solution, Chain Length and Treatment with Mild Reducing Agents. *J.*
51 *Electroanal. Chem.* **2011**, *661*, 90–99.
52
53
54
55
56
57
58
59
60

- 1
2
3
4 (26) Cometto, F. P.; Ruano, G.; Ascolani, H.; Zampieri, G. Adlayers of Alkanedithiols on
5 Au(111): Effect of Disulfide Reducing Agent. *Langmuir* **2013**, *29*, 1400–1406.
6
7 (27) Soler, J. M.; Artacho, E.; Gale, J. D.; García, A.; Junquera, J.; Ordejón, P.; Sánchez-Portal,
8 D. The SIESTA Method for Ab Initio Order-N Materials Simulation. *J. Phys. Condens. Matter*
9 **2002**, *14*, 2745.
10
11 (28) Perdew, J. P.; Burke, K.; Ernzerhof, M. Generalized Gradient Approximation Made Simple.
12 *Phys. Rev. Lett.* **1996**, *77*, 3865–3868.
13
14 (29) Henkelman, G.; Jónsson, H. Improved Tangent Estimate in the Nudged Elastic Band
15 Method for Finding Minimum Energy Paths and Saddle Points. *J. Chem. Phys.* **2000**, *113*, 9978–
16 9985.
17
18 (30) Henkelman, G.; Uberuaga, B. P.; Jónsson, H. A Climbing Image Nudged Elastic Band
19 Method for Finding Saddle Points and Minimum Energy Paths. *J. Chem. Phys.* **2000**, *113*, 9901–
20 9904.
21
22 (31) Frisch M. J. et.al. Gaussian 09, Revision D.01, Gaussian, Inc., Wallingford CT, 2009.
23
24 (32) Tomasi, J.; Mennucci, B.; Cammi, R. Quantum Mechanical Continuum Solvation Models.
25 *Chem. Rev.* **2005**, *105*, 2999–3093.
26
27 (33) Sun, F.; Castner, D. G.; Mao, G.; Wang, W.; McKeown, P.; Grainger, D. W. Spontaneous
28 Polymer Thin Film Assembly and Organization Using Mutually Immiscible Side Chains. *J. Am.*
29 *Chem. Soc.* **1996**, *118*, 1856–1866.
30
31 (34) Laibinis, P. E.; Whitesides, G. M.; Allara, D. L.; Tao, Y. T.; Parikh, A. N.; Nuzzo, R. G.
32 Comparison of the Structures and Wetting Properties of Self-Assembled Monolayers of n-
33 Alkanethiols on the Coinage Metal Surfaces, Copper, Silver, and Gold. *J. Am. Chem. Soc.* **1991**,
34 *113*, 7152–7167.
35
36 (35) Fabianowski, W.; Coyle, L. C.; Weber, B. A.; Granata, R. D.; Castner, D. G.; Sadownik, A.;
37 Regen, S. L. Spontaneous Assembly of Phosphatidylcholine Monolayers via Chemisorption onto
38 Gold. *Langmuir* **1989**, *5*, 35–41.
39
40 (36) Kawasaki, M.; Iino, M. Self-Assembly of Alkanethiol Monolayers on Ag–Au(111) Alloy
41 Surfaces. *J. Phys. Chem. B* **2006**, *110*, 21124–21130.
42
43 (37) Streitwieser, A.; McKeown, A. E.; Hasanayn, F.; Davis, N. R. Basicity of Some Phosphines
44 in THF. *Org. Lett.* **2005**, *7*, 1259–1262.
45
46 (38) Wang, C.; Qi, C. Mechanistic Insights into N- or P-Centered Nucleophile Promoted Thiol–
47 vinylsulfone Michael Addition. *Tetrahedron* **2013**, *69*, 5348–5354.
48
49 (39) Dmitrenko, O.; Thorpe, C.; Bach, R. D. Mechanism of SN₂ Disulfide Bond Cleavage by
50 Phosphorus Nucleophiles. Implications for Biochemical Disulfide Reducing Agents. *J. Org.*
51 *Chem.* **2007**, *72*, 8298–8307.
52
53
54
55
56
57
58
59
60

- 1
2
3 (40) Patrito, E. M.; Olivera, P. P.; Sellers, H. On the Nature of the $\text{SO}_4^{2-}/\text{Ag}(111)$ and
4 $\text{SO}_4^{2-}/\text{Au}(111)$ Surface Bonding. *Surf. Sci.* **1997**, *380*, 264–282.
5
6
7 (41) Paredes Olivera, P.; Patrito, E. M.; Sellers, H. Adsorption of Sulfate, Bisulfate and Sulfuric
8 Acid on Silver Surfaces: A Theoretical Study. *Surf. Sci.* **1998**, *418*, 376–394.
9
10 (42) Jewell, A. D.; Tierney, H. L.; Sykes, E. C. H. Gently Lifting Gold's Herringbone
11 Reconstruction: Trimethylphosphine on Au(111). *Phys. Rev. B* **2010**, *82*, 205401.
12
13 (43) Lustemberg, P. G.; Martiarena, M. L.; Martínez, A. E.; Busnengo, H. F. The Reaction
14 Pathways for HSCH₃ Adsorption on Au(111): A Density Functional Theory Study. *Langmuir*
15 **2008**, *24*, 3274–3279.
16
17 (44) Chaudhari, V.; Kotresh, H. M. N.; Srinivasan, S.; Esaulov, V. A. Substitutional Self-
18 Assembly of Alkanethiol and Selenol SAMs from a Lying-Down Doubly Tethered Butanedithiol
19 SAM on Gold. *J. Phys. Chem. C* **2011**, *115*, 16518–16523.
20
21 (45) Ferreira, V. C.; Silva, F.; Abrantes, L. M. Electrochemical and STM Study of ω -
22 Alkanedithiols Self-Assembled Monolayers. *Chem. Biochem. Eng. Q.* **2009**, *23*, 99–106.
23
24 (46) Lukesh III, J. C.; VanVeller, B.; Ronald T. Raines, R. T. Thiols and Selenols as Electron-
25 Relay Catalysts for Disulfide-Bond Reduction. *Angew. Chem.* **2013**, *125*, 13139–13142.
26
27 (47) Creczynski-Pasa, T. B.; Daza Millone, M. A.; Munford, M. L.; de Lima, V. R.; Tiago O.
28 Vieira, T. O.; Guillermo A. Benitez, G. A.; Pasa, A. A.; Salvarezza, R. C.; Vela, M. E. Self-
29 assembled Dithiothreitol on Au Surfaces for Biological Applications: Phospholipid Bilayer
30 Formation. *Phys. Chem. Chem. Phys.* **2009**, *11*, 1077–1084.
31
32 (48) Cometto, F. P.; Macagno, V. A.; P. Paredes-Olivera, P.; Patrito, E. M.; Ascolani, H.;
33 Zampieri, G. Decomposition of Methylthiolate Monolayers on Au(111) Prepared from Dimethyl
34 Disulfide in Solution Phase. *J. Phys. Chem. C*, **2010**, *114*, 10183–10194.
35
36 (49) Cometto, F. P.; Calderón, C. A.; Morán, M.; Ruano, G.; Ascolani, H.; Zampieri, G.;
37 Paredes-Olivera, P.; E. M. Patrito, E. M. Formation, Characterization, and Stability of
38 Methaneselenolate Monolayers on Au(111): An Electrochemical High-Resolution Photoemission
39 Spectroscopy and DFT Study. *Langmuir*, **2014**, *30*, 3754–3763.
40
41 (50) Burns, J. A.; Whitesides, G. M. Predicting the Stability of Cyclic Disulfides by Molecular
42 Modeling: “Effective Concentrations” in Thiol-Disulfide Interchange and the Design of Strongly
43 Reducing Dithiols. *J. Am. Chem. Soc.* **1990**, *112*, 6296–6303.
44
45
46
47
48
49
50
51
52
53
54
55
56
57
58
59
60

TOC

